İSTANBUL UNIVERSITY CERRAHPAŞA

ORIGINAL ARTICLE
Electrica 2024; 24(1): 183-192

Investigation With Rule-Based Controller of Energy Consumption of Parallel Hybrid Vehicle Model in Different States of Charge

Yılmaz Seryar Arıkuşu[1], Nevra Bayhan[2], Hasan Tiryaki[2]

[1]Department of Electrical Engineering, Manisa Celal Bayar University Hasan Ferdi Turgutlu Faculty of Technology, Manisa, Turkey
[2]Department of Electrical and Electronics Engineering, Istanbul University-Cerrahpaşa Faculty of Engineering, Istanbul, Turkey

Cite this article as: Y. S. Arıkuşu, N. Bayhan and H. Tiryaki, "Investigation with rule-based controller of energy consumption of parallel hybrid vehicle model in different states of charge," *Electrica*, 24(1), 183-192, 2024.

ABSTRACT

In this study, a parallel hybrid electric vehicle has been modeled and a new rule-based and battery-priority control method has been proposed, which will reduce fuel consumption and carbon emission values to minimum values. This control method is based on running the electric motor more and operating the internal combustion engine in the most efficient region. In the proposed control method, it is also ensured that the electric motor is operated as a generator. The control method is used in New European Driving Cycle (NEDC), ECE-15 (Urban Driving Cycle), and in Extra Urban Driving Cycle (EUDC) driving cycle conditions. In this study, two different simulation studies are achieved in accord with the critical state of charge (SOC) of the battery. The SOC value is selected 55% and 65% for its effect on fuel consumption in these driving cycles. According to the results, the parallel hybrid electric vehicle which has a 65% SOC value, gasoline efficiency becomes executed 35.7% inside the NEDC cycle, 25.3% in the EUDC cycle, and 52.3% in the ECE-15 cycle. Furthermore, for the parallel hybrid electric vehicle with a 55% SOC value, fuel efficiency is 29.3% in the ECE-15 driving cycle, 17.6% in the NEDC driving cycle, and 9.6% in the EUDC cycle. The proposed control approach yields the parallel hybrid vehicle's fuel usage and fuel efficiency.

Index Terms— Fuel consumption minimization, hybrid electric vehicle (HEV), modeling, rule-based control algorithm, simulation

I. INTRODUCTION

Nowadays, the carbon emissions of countries have been increasing rapidly as a result of increasing environmental pollution and global warming. The predominant causes of the rise in carbon emissions are the utilization of fossil fuel resources in the transportation and energy sectors [1]. It is possible to significantly reduce these emissions by expanding electric vehicles in the transportation sector and renewable energy sources in electricity generation [2]. It is also possible to reduce carbon emissions by developing methods that will enable vehicles that consume less energy to travel longer and use internal combustion engines (ICEs) less. Therefore, hybrid vehicles have been developed that will enable both electric motors (EMs) and ICE to operate simultaneously. Various techniques have been established in literature to guarantee the fuel efficiency of hybrid vehicles. The main ones of these methods are rule-based, fuzzy logic-based control methods, equivalent energy minimization method and metaheuristic algorithms are used.

The rule-based control methods in the literature are created according to the power demanded in the driving cycle. In the literature, a rule-based controller was created considering several situations, including starting the EM only when low performance is required and operating the EM and the ICE when high performance is desired [3-14]. Rule-based methods have the benefit of being simple. Another benefit is that it does not require any forward-looking knowledge of driving. In addition, the fuzzy logic control system used in hybrid vehicles provides convenience in analyzing the complex structure of the vehicle by being formed from fuzzy sets. The fuzzy logic control system is used to adjust the powertrains and provide the optimum fuel efficiency [15-17]. The required power torque is obtained by taking the state of charge as an input. In order to reduce fuel consumption, the efficiencies of the components of the vehicle (ICE, EM, gearbox, and battery) are optimally adjusted using the fuzzy logic method [15-17]. Moreover, an adaptive neuro-fuzzy inference system (ANFIS) is used for a hybrid energy-efficient vehicles [18-19]. Adaptive neuro-fuzzy inference system offers good performance and enhances hybrid

Corresponding author:
Nevra Bayhan

E-mail:
nevra@iuc.edu.tr

Received: October 18, 2023

Accepted: November 12, 2023

Publication Date: January 31, 2024

DOI: 10.5152/electrica.2024.23167

electric vehicles' fuel economy. However, real-time implementation of energy management systems based on ANFIS and fuzzy control is complex and challenging.

On the other hand, metaheuristic algorithms are also used for energy efficiency in hybrid vehicles [20-21]. Results from metaheuristic algorithms have been found to maximize energy efficiency and reduce fuel use [20-21]. However, metaheuristic algorithms are difficult to adapt to real systems because they provide stochastic solutions.

In this article, it has been studied on the conversion of a gasoline light commercial vehicle to a hybrid electric vehicle in order to develop fuel efficiency-enhancing and innovative technologies for ICE vehicles. Therefore, a new rule-based and battery-priority control method has been proposed, and a parallel hybrid electric vehicle was developed to minimize fuel consumption and carbon emission values. The aim of this control strategy is predicated on using the ICE in its most efficient zone and running the EM more.

The novelties in this study are as follows.

- A rule-based and battery-priority fuel consumption control algorithm has been created to keep the propulsion systems of hybrid vehicles at the highest level, control the crucial battery status, and maintain the efficiency of the ICE.
- Fuel minimization has been achieved by creating 11 different rule methods in New European Driving Cycle ((NEDC), ECE-15, and Extra Urban Driving Cycle (EUDC) cycles. In addition, the fuel consumption is 3.6 L/100 km in the proposed algorithm for the EUDC cycle with 65% state of charge (SOC), whereas the fuel consumption of research of [17] is 5.4 L/100 km in the EUDC cycle.
- When the 55% SOC value is selected close to the minimum value, the effect on fuel minimization was examined and fuel efficiency was obtained even though ICE was used more.

The rest of the article is as follows: model of hybrid vehicle is discussed in Section II, fuel consumption control algorithm is explained in Section III, simulation and discussion are discussed in Section IV and conclusion is explained in Section V.

II. MODEL OF HYBRID VEHICLE

In this article, the parallel hybrid electric vehicle model and energy control method have been studied. A parallel hybrid electric vehicle consists of an ICE and an EM. The model structure of the parallel hybrid vehicle (PHEV) is shown in Fig. 1. Since ICE and EM are connected in parallel, it is considered as a PHEV. In a PHEV, the EM is driven when the demand power is low, and the ICE is driven when the demand power is high. The advantages of the PHEV are as follows: the ICE provides direct drive under suitable conditions and the EM creates an extra energy source by using it as a generator.

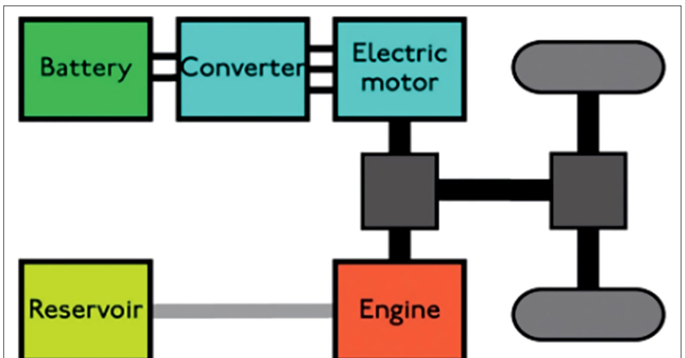

Fig. 1. Parallel hybrid vehicle [21].

The simulation study of the PHEV model is shown in Fig. 2. Here, driving cycle, vehicle model, transmission, EM model, and ICE model have been used for simulation. The simulation has been done using the MATLAB QSS toolbox library [22].

A. Driving Cycle

Time-dependent speed-time graphics are called driving cycles, which are created to ascertain and assess a vehicle's fuel efficiency and emissions values. Driving cycles represent the traffic conditions in which the vehicle will be used in order to determine fuel consumption and carbon emissions. In this study, NEDC, ECE-15, and EUDC have been used to examine the fuel consumption control method. With these driving cycles, it is aimed to reduce the carbon emission values with the proposed control method.

B. Forces Acting on the Vehicle

When a vehicle is in motion, a resistive force F_T occurs. These resistance forces are the forces that the vehicle must overcome for movement. The resistance forces consist of the rolling resistance force (F_r), the force due to the airflow on the body of the vehicle (F_{air}), the hill resistance (F_i), and acceleration force (F_a) required for the acceleration of the vehicle The connection between these resistive forces is given in (1)

$$F_T = F_r + F_i + F_{air} + F_a \quad (1)$$

Wheel rolling resistance occurs in front of the wheel contact center against rolling due to the elastic structure of the wheel. Rolling resistance (F_r) as the following term:

$$F_r = mgcos(\theta)C_{st} \quad (2)$$

Air resistance force (F_{air}) is as follows:

$$F_{air} = 0.5pAC_DV^2 \quad (3)$$

where, p is density of air, A is the cross-sectional area of the vehicle, V is velocity, and C_D is aerodynamic coefficient.

Hill resistance (F_i) depends on vehicle mass and road slope is given as

$$F_i = mgsin(\theta) \quad (4)$$

Acceleration force (F_a) is given in (5)

$$F_a = ma \quad (5)$$

where a is acceleration.

C. Internal Combustion Engine

In this study, the specific fuel consumption map of the ICE was created with the MATLAB QSS [22] toolbox library. The specific fuel consumption map is created according to the engine power of 70 kW, which is the speed of the driving cycle and represents the gram value of the fuel that the ICE should consume per kWh of work with the rule-based control method.

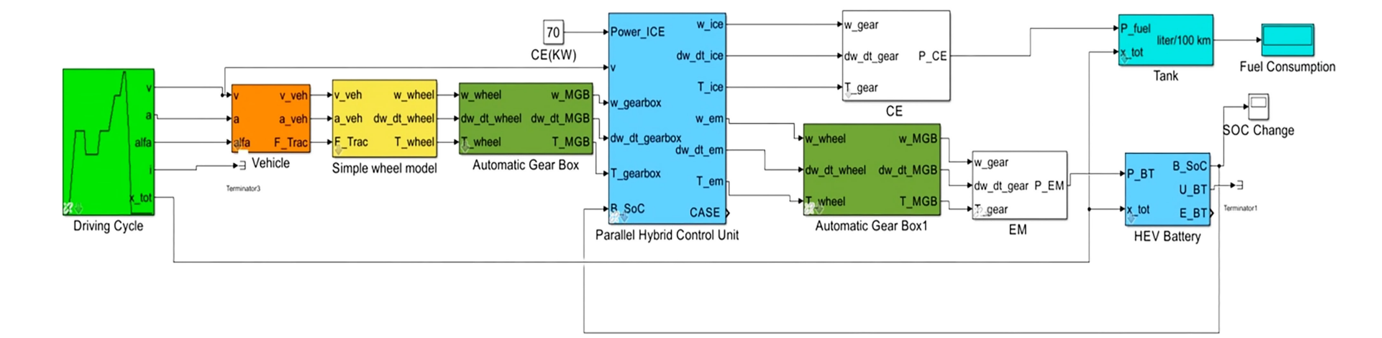

Fig. 2. Design of parallel hybrid vehicle.

D. Electric Motor

Electric motors are devices that generate the driving torque necessary for the vehicle's movement by transforming the electrical energy from the battery into mechanical energy. Electric motor was also created with the MATLAB QSS toolbox library [22]. The positive part of EM shows the operating state of the EM. The negative part of EM refers to the places where it is used as a generator. With the rule-based control algorithm, the speed and torque values of the EM will be clustered depending on the driving cycle.

E. Design of Battery Model

In hybrid electric vehicles, the battery supplies the energy required to run the EM. The battery model includes battery charge, battery discharge, voltage variation, and current generation. The battery equations used in the simulation are given in (6) and (7)

$$P_s(t)=V_{OC}\left(SOC(t)I(t)\right) \tag{6}$$

$$Pbat(t)=V_{OC}\left(SOC(t)\right)I(t)-I(t)^2R_i\left(SOC(t),sign(Pbat)\right) \tag{7}$$

F. Power Transmission

The gearbox is one of the most crucial powertrains for hybrid electric automobiles. The gearbox enables vehicles to operate safely and efficiently in different speeds, torques, and road conditions. Thanks to the manual gearbox it was possible to transmit mechanical work between different torque levels or rotational speed. The manual gearbox was created with the MATLAB QSS toolbox [22].

III. FUEL CONSUMPTION CONTROL METHOD

In this study, a rule-based control method is proposed to obtain fuel efficiency in parallel hybrid electric vehicles. The reason for using a rule-based algorithm is that it is practical and strategies based on human observation can be developed easily. Thanks to the control method proposed here, the operating range of the ICE is reduced by adjusting the engine transitions in the vehicle. In addition, the EM receives the extra torque produced by the ICE, which enables the EM to act as a generator and conserve energy.

In this study, the energy consumption control for PHEV is developed by taking into account the actual disparity between the power required by the driver at any given time and the power generated by the ICE. When there is a significant need for power, the ICE is started. When there is a low demand for power compared to the power of the ICE, the EM is used as the primary power source. Apart from the power demanded for the operation of the EM, SOC is also taken into account. An energy control method system has been developed according to the minimum and maximum constraints of the SOC value. The EM and battery are modeled to enable the vehicle to take off Additionally, until the vehicle reaches the speed at which the ICE runs more effectively, it will be propelled by the EM. Thus, ICE will be turned off while the vehicle is in motion. It will be prevented from operating in low-speed regions where it operates inefficiently, and engine efficiency will be ensured. Therefore, a flowchart algorithm for PHEV energy controller has been developed and is shown in Fig. 3. The innovation in the rules shown in Fig. 3 for the hybrid electric vehicle is the energy gain and the operation of the ICE with the control algorithm method where optimum points. Thus, energy consumption is kept to a minimum value in the proposed control method. In Fig. 3, v is velocity, v_{lim} is the maximum speed of the EM, T is torque value in gearbox, and T_{lim} is the maximum torque value of the EM. SOC_{min} is the maximum torque value of the EM and SOC_{max} is the maximum battery state of charge. The lower and upper limit values which is speed and torque of the vehicle parameter values of the EM are given in Table I. In simulation, it is performed according to the limit values given in Table I of the energy control method. During the simulation, if the values from the driving cycle are within the limits that the EM can operate, the EM runs. If the values from the driving cycle are not within the limits of the EM, ICE operates.

When Table I and Fig. 3 are examined, there are three basic input parameters that determine the operating status of the hybrid vehicle. These are SOC, torque, and speed values.

Examining Fig. 3, the following results are obtained:

where $SOC < SOC_{min}$, $T < T_{lim}$, and $v < v_{lim}$, it operates ICE. Torque and speed values are ideal for the EM, but the ICE engine must operate at an optimum level because the SOC value is less than the minimum value. In addition, the mechanical energy produced by ICE is transmitted to the EM, and it is ensured to operate as a generator. Thus, the battery will be charged. In the second rule, $SOC < SOC_{min}$, $T < T_{lim}$, and $v > v_{lim}$, the ICE motor works at the optimum level because SOC value is below the minimum value, while speed value is above the maximum value. The battery is charged because the ICE motor transmits excess energy to the EM. In the third rule, $SOC > SOC_{min}$, $T < T_{lim}$, and $v > v_{lim}$, the EM works because the SOC value is greater than the minimum value, and thus the speed and torque values are ideal for the operation of the EM. In the fourth rule, $SOC > SOC_{max}$, $T < T_{lim}$, and $v < v_{lim}$, EM is running because the demand power and torque is small, and the SOC value is high.

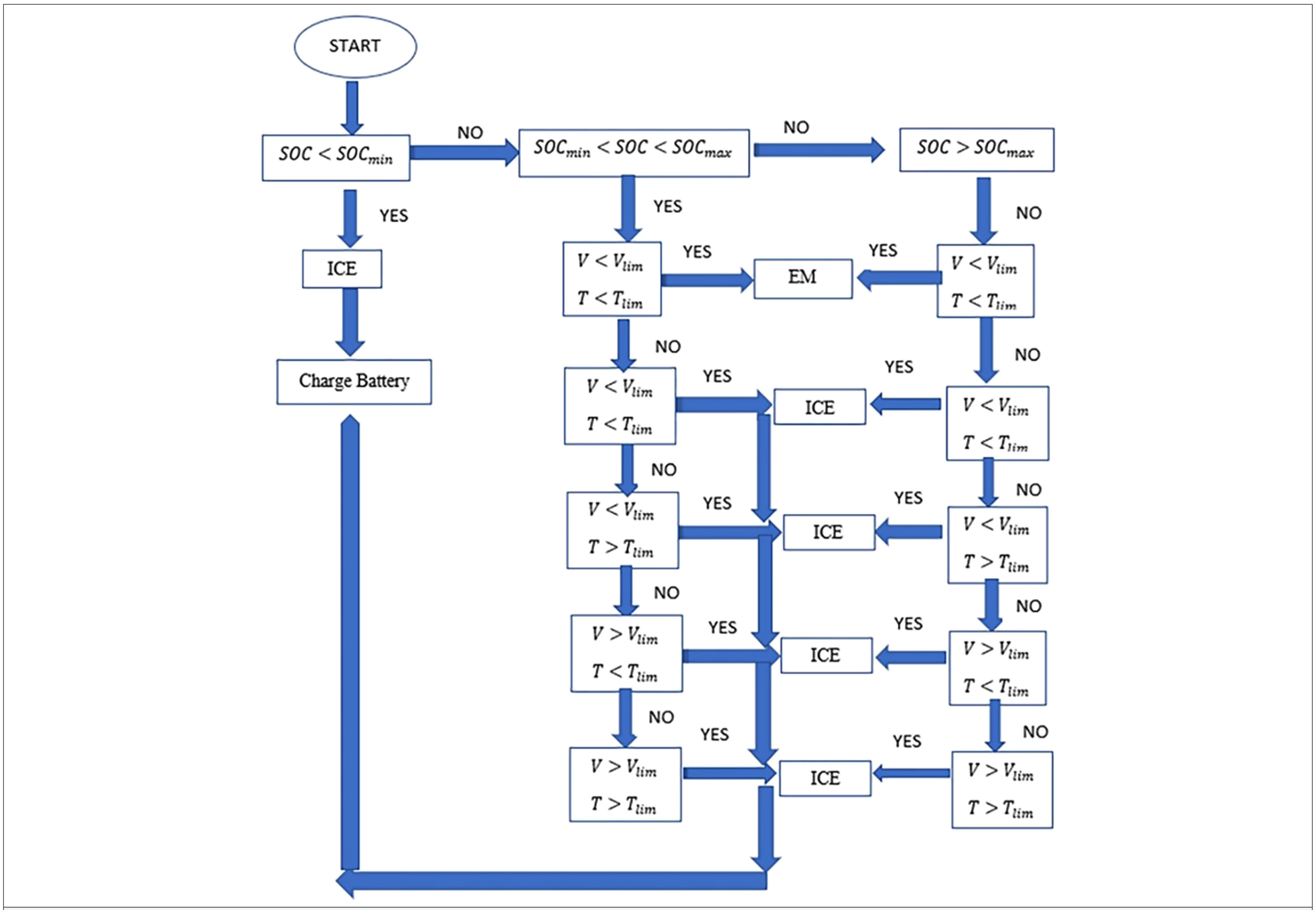

Fig. 3. Rule-based control method flowchart.

In the fifth rule, $SOC > SOC_{min}$, $T < T_{lim}$, and $v > v_{lim}$, the ICE is running. In addition, the ICE supports the EM and enables the battery to be charged. In the sixth rule, $SOC < SOC_{max}$, $T < T_{lim}$, and $v > v_{lim}$, ICE is working since the SOC value is not at the maximum level, and ICE additionally aids the EM in charging the battery. In the seventh rule, $SOC > SOC_{max}$, $T < T_{lim}$, and $v > v_{lim}$, the ICE motor is started. Here, the battery does not charge because the SOC is greater than the maximum value. In the eighth rule, $SOC > SOC_{min}$, $T > T_{lim}$, and $v < v_{lim}$, ICE works. In addition, the EM is a generator since the ICE transfers any excess mechanical energy to it. Thus, the battery is charged. In the ninth rule, $SOC < SOC_{max}$, $T > T_{lim}$, and $v < v_{lim}$, ICE runs due to the high torque value demanded. The battery is charged because the SOC value is less than the maximum value. In the tenth rule, $SOC > SOC_{max}$, $T > T_{lim}$, and $v < v_{lim}$, ICE works. In the eleventh rule, $SOC > SOC_{max}$, $T > T_{lim}$, and $v > v_{lim}$, ICE works because torque and speed values are greater than values of EM. The vehicle parameters used to simulate the rule-based energy management strategy are given in Table II. For the simulation made using the values in Table II, driving cycles are used as the input values [15]. According to the power to be obtained from the driving cycle, the rule-based control method is used to determine how much fuel the vehicle consumes on the specific fuel consumption map. In this study, a

TABLE I. SOC, T_{lim} VE v_{lim} VALUES.

SOC_{min} (%)	SOC_{max} (%)	v_{lim} (m/s)	T_{lim} (Nm)
45	70	40	80

TABLE II. VEHICLE PARAMETERS [15]

Parameters	Value
Total Mass (kg)	2000
Aerodynamic coefficient	0.31
Vehicle surface area (m^2)	3.11
Coefficient of rolling	0.009
Wheel radius (mm)	300.3
ICE engine power (kW)	70
EM engine power (kW)	60
Gear ratios	[3.31, 1.91, 1.26, 0.94, 0.76]
Differential atio	4.16

EM, electric motor; ICE, internal combustion engine.

simulation study of the energy control strategy of a PHEV was carried out using the vehicle parameters in ECE-15, NEDC, and EUDC driving cycles in Table II.

IV. SIMULATION RESULTS AND DISCUSSION

In this simulation study, SOC values were selected as 65% and 55%. The reason for this is to examine the effect of the control method on vehicle performance and fuel consumption by choosing the SOC value in the range close to the maximum and minimum. In addition, in the simulation study, first, the percentage value of the SOC value of the vehicle battery was chosen as 65 in the ECE-15 driving cycle. The reason for choosing the SOC value as 65 is that the EM can be used more. Fig. 4a shows how the battery changes over time when operated in the ECE-15 driving cycle. Since the speed and power values of the ECE-15 driving cycle are low, it is seen in Fig. 4 that the energy increase is very small. The power generated using the rule-based control method during the ECE-15 driving cycle for the ICE and the EM is illustrated in Fig. 4b. When Fig. 4b is examined carefully, it is seen that the ICE engine produces more power with the increase in vehicle speed. Since the speed value is low in the ECE-15 cycle, the EM motor works more. In Fig. 4b, it is seen that the power value of the EM is constantly changing. In this context, it is seen that the rule-based control algorithm allows the EM to operate at low power demands. The negative power in Fig. 4b, on the other hand, transmits some of the power produced by the ICE after working at high power to the EM, enabling the EM to work as a generator. In this context, it shows that the EM charges the battery. The operating points of the EM are shown in Fig. 4c. When Fig. 4c is examined, it is seen that the EM works continuously in efficient regions. The reason for this is that the speed and torque values are low as the ECE-15 cycle including the urban cycle. The gram value of the fuel used when the ICE engine is running is shown in Fig. 4d. The red dots in Fig. 4d show the grams of fuel when the ICE engine is running. It is seen that the red dots are clustered at the most optimum and lowest points. Thus, it is observed that ICE is used less frequently.

In the rule-based energy control management algorithm of the EUDC driving cycle, the SOC value was selected as 65%, and the simulation results were examined. The variation of the SOC value over time using the energy control method in the EUDC cycle is shown in Fig. 5a. Although the EUDC has a non-urban loop structure, it is seen in Fig. 5a that the battery has decreased to 64.4% according to the demanded power value. This is because the speed value and torque value are used at the maximum level. In addition, it has been observed that the ICE is used intensively in the 350th second, and it charges the battery by providing power support to the EM. The amount of power obtained according to the rule-based control method in the EUDC driving cycle of ICE and EM is given in Fig. 5b. It is seen that the ICE power in the EUDC cycle, which has high speed values, is higher than the ECE-15 cycle. In Fig. 5c, the operating points of the EM are shown with blue dots. When Fig. 5c is examined, it is observed that the EM works less in efficient regions compared to the ECE-15 cycle. The reason is that the EUDC cycle includes the extra-urban cycle, so the speed and torque values are high. In addition, it is seen that the negative power point is more in Fig. 5c because EM is used as a generator since it is high power. The gram value of the fuel used when the ICE engine is running is shown in Fig. 5d.

A simulation of the energy control strategy is carried out by selecting the SOC value of a PHEV under the NEDC driving cycle by 65% and using the vehicle parameters in Table III. The NEDC driving cycle consists of ECE-15 and EUDC driving cycle. The change of the SOC value over time using the energy control method in the NEDC cycle is shown in Fig. 6a. As evident from Fig. 6a, the battery is used more because the first 800 seconds of the NEDC cycle consist of ECE-15 cycle. Since the EUDC cycle is active after 800 seconds, the battery is used less. As a result, it is seen in Fig. 6a that the battery has decreased to 64.4% according to the demanded power value. The amount of power obtained according to the rule-based control method in the NEDC driving cycle of the ICE and the EM is illustrated in Fig. 6b. When Fig. 6b is examined carefully, there are decreases in the battery due to the use of EM where there is low power and torque demand in the NEDC driving cycle. In the last part of the driving cycle, where ICE is used intensively, EM is used as a generator; therefore, the SOC value increases. Fig. 6c shows at what speed and how much torque the electrical power values work in the NEDC cycle. The operating

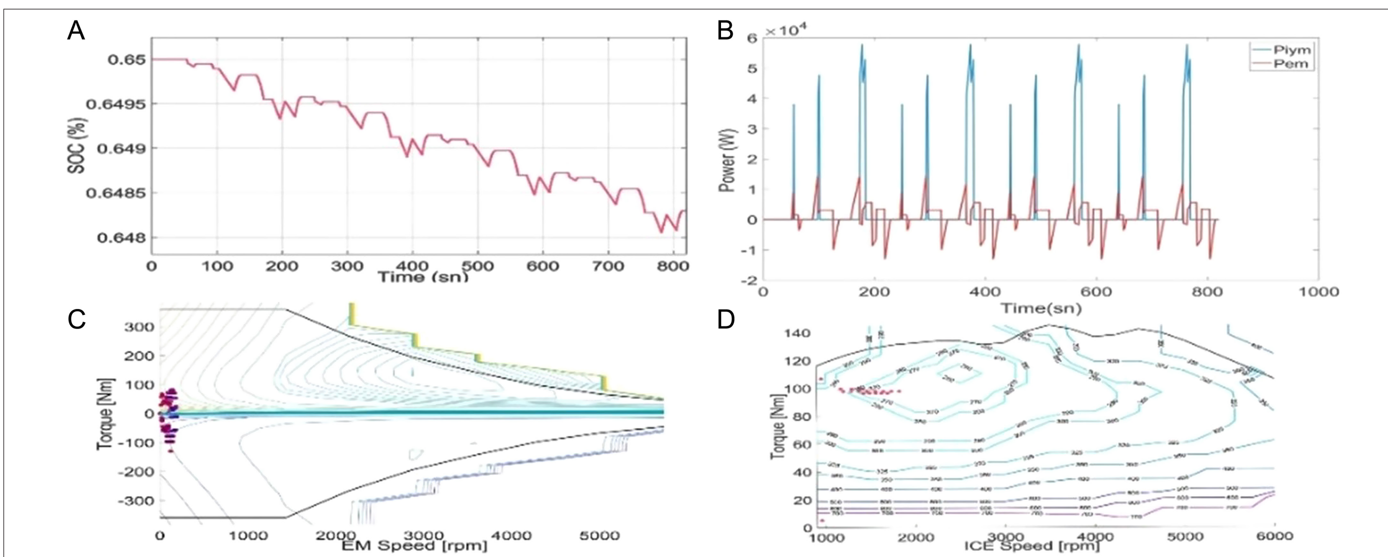

Fig. 4. (a) 65% SOC value in ECE-15 cycle. (b) ICE and EM power values for 65% SOC. (c) EM speed–torque values for 65% SOC. (d) Specific fuel consumption map for 65% SOC.

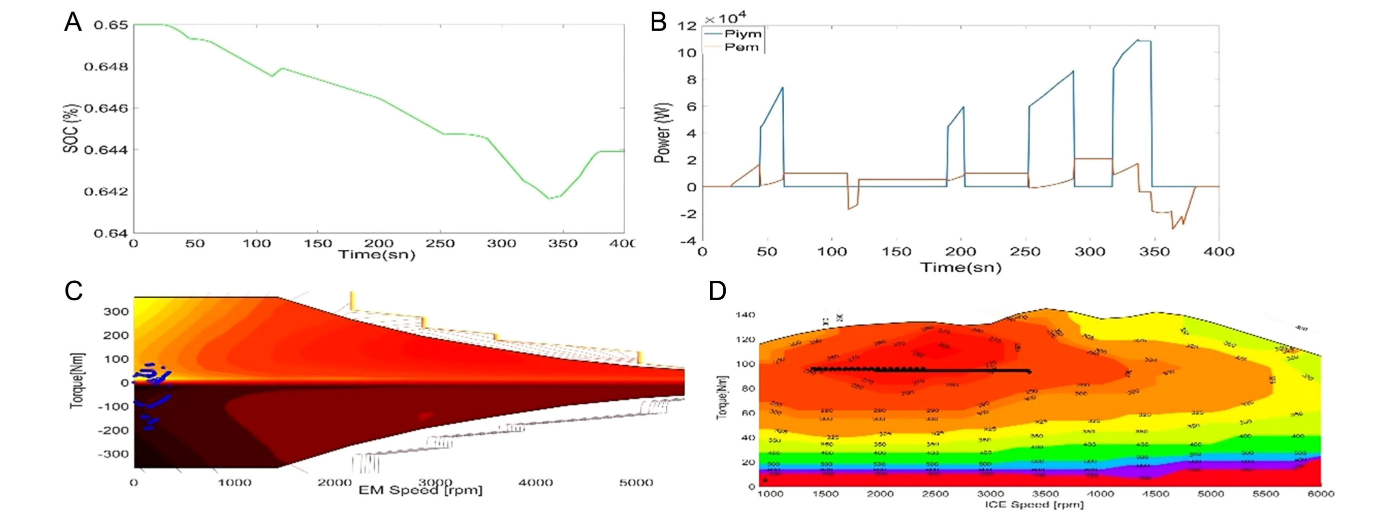

Fig. 5. (a) 65% SOC value in EUDC cycle. (b) ICE and EM power values for 65% SOC. (c) EM speed–torque values for 65 SOC. (d) Specific fuel consumption map for 65% SOC.

points of the EM are shown with red dots in the efficient regions in Fig. 6c. Clustering of EM where low power is required in the NEDC loop indicates the correct operation of the control method system because the control system requires EM to operate when the vehicle requests low power. Fig. 6c also shows that the EM produces too much negative torque. This situation indicates that the EM is working as a generator. The gram value of the fuel used when the ICE engine is running is shown in Fig. 6d. The black dots in Fig. 6d are the operating points of the ICE. Thus, it was observed that ICE operating points are clustered at the lowest points as in other cycles.

In this part of the simulation study, the effect of the rule-based control algorithm on the fuel performance was investigated by selecting the SOC value of 55% in the ECE-15, EUDC, and NEDC cycles. The variation of the SOC value with time in the ECE-15 cycle is given in Fig. 7a. The ICE and EM power values are given in Fig. 7b. When Fig. 7a and Fig. 7b are

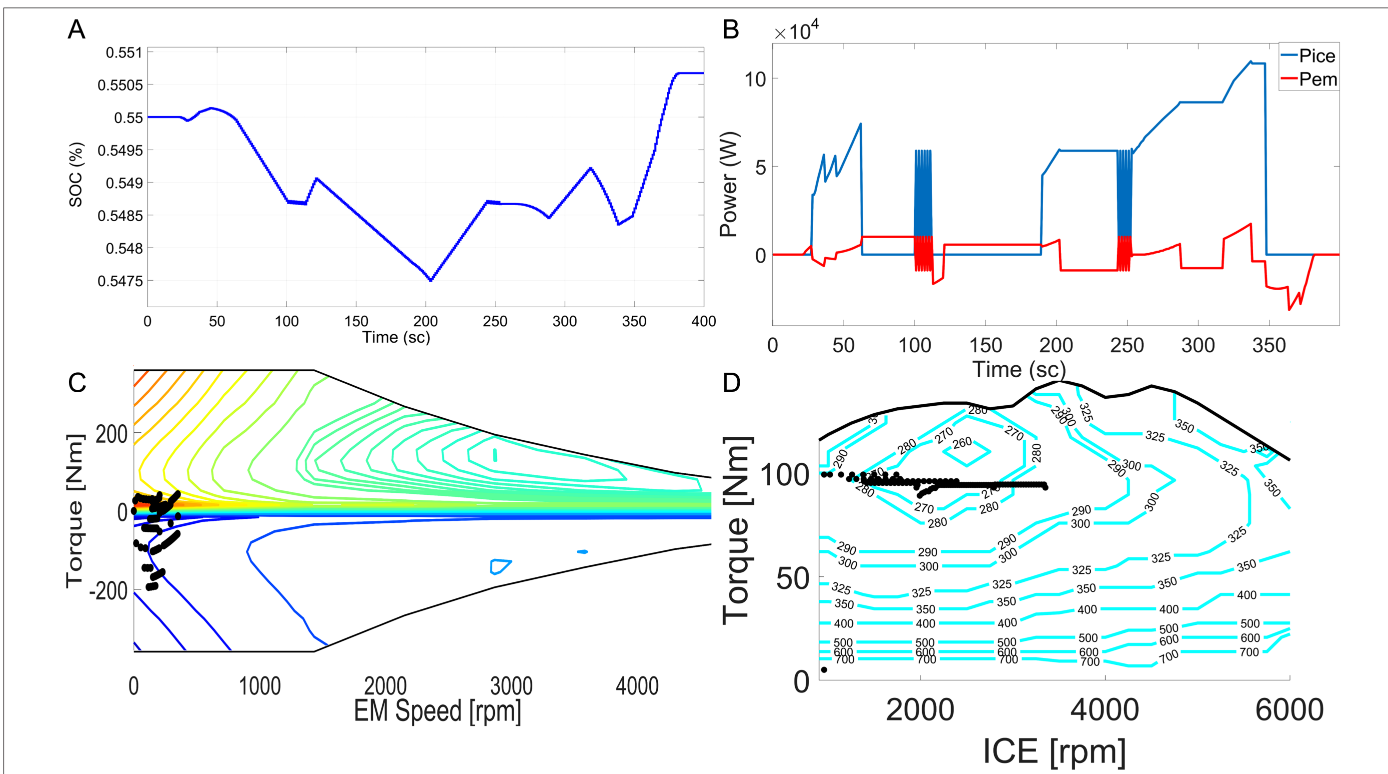

Fig. 8. (a) 55 SOC value in EUDC cycle for 55%. (b) ICE and EM power values for 55%. (c) EM speed–torque values for 55% SOC. (d) Specific fuel consumption map for 55% SOC.

TABLE III. SPECIFIC FUEL CONSUMPTION FOR VEHICLES

Specific Fuel Consumption (L/100 km)			
	NEDC	**ECE-15**	**EUDC**
Conventional vehicle	7.262	7.591	7.07
Parallel hybrid vehicle (%65 SOC)	3.549	3.441	3.6
Parallel hybrid vehicle (%55 SOC)	5.979	5.363	6.391

NEDC, New European Driving Cycle; ECE-15, Urban Driving Cycle; EUDC, Extra Urban Driving Cycle.

examined, it is seen that ICE is used more, although there is less power demand in the ECE-15 driving cycle. The excess mechanical energy produced by ICE is transmitted to the EM which enables it to operate as a generator. Thus, the change in the SOC value in Fig. 7a shows that the battery charges. The battery value is charged according to the amount of power obtained. At the end of the ECE-15 cycle, it is observed that the SOC value is higher than the initial state. The speed–torque graph of EM according to 55% SOC value in ECE cycle is given in Fig. 7c. In Fig. 7c, the battery is charged more because the EM is more clustered at the negative points. The specific fuel consumption map of ICE is illustrated in Fig. 7d. Despite the intensive use of ICE, it has been observed that the specific fuel consumption is clustered at minimum points.

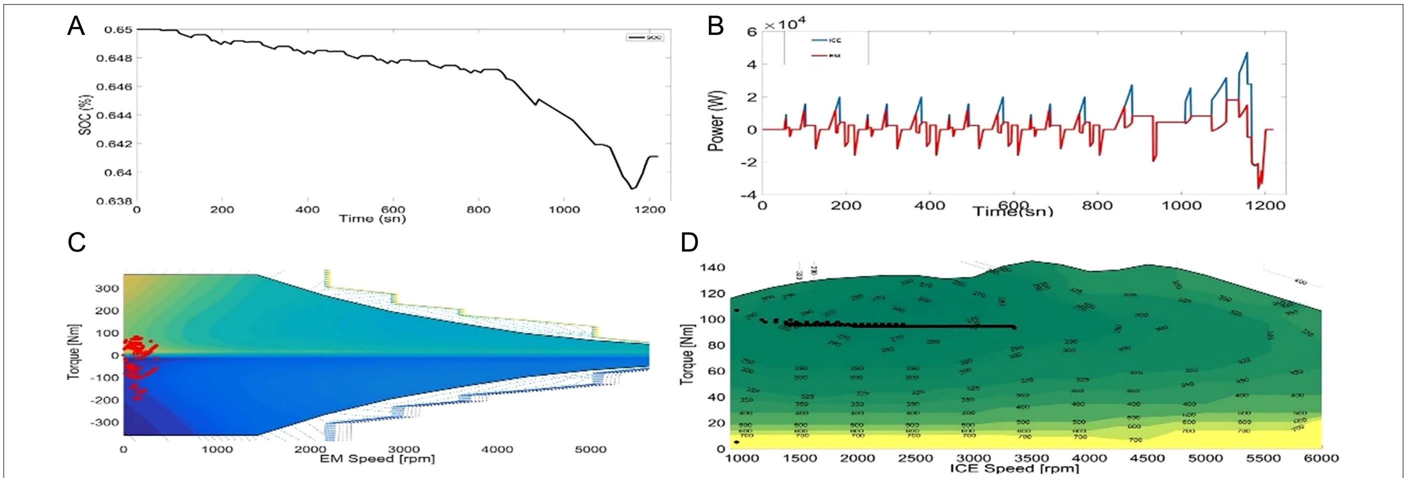

Fig. 6. (a) 65% SOC value in NEDC cycle. (b) ICE and EM power values for 65% SOC. (c) EM speed–torque values for 65% SOC. (d) Specific fuel consumption map for 65% SOC.

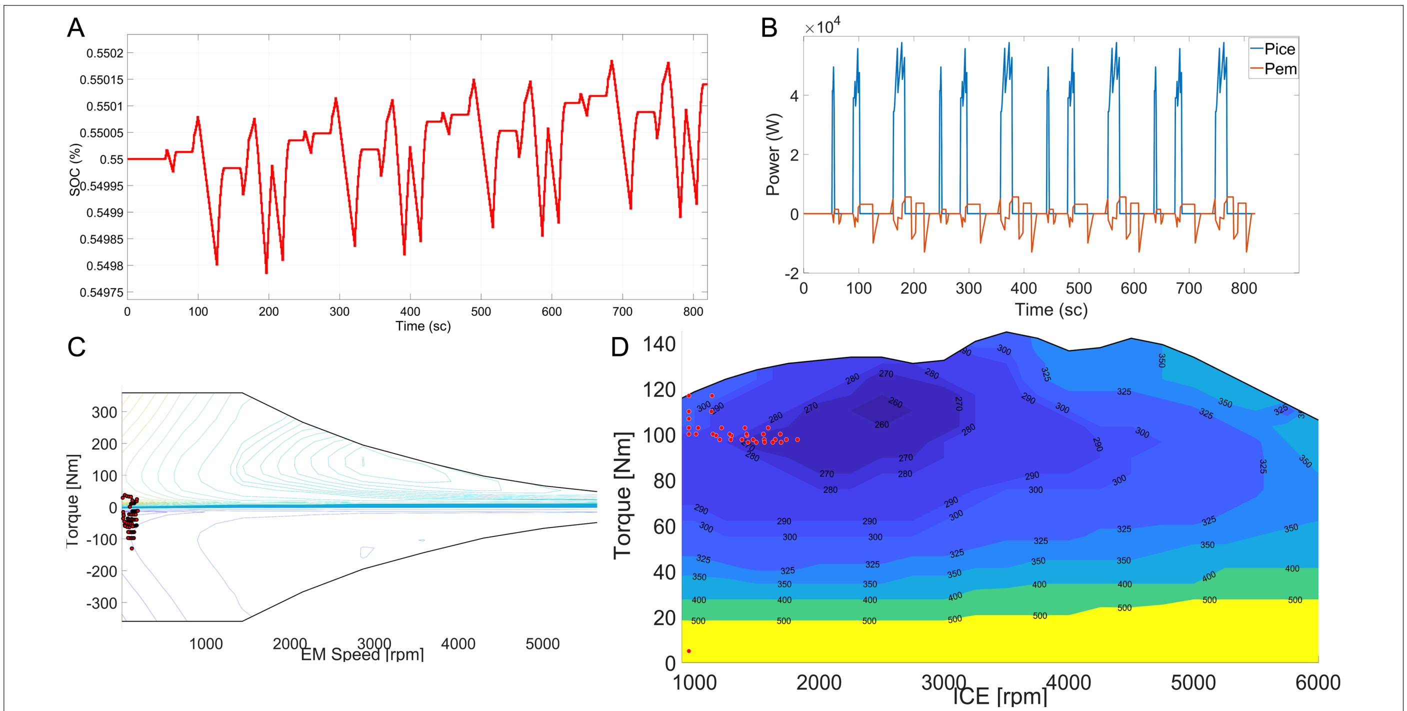

Fig. 7. (a) 5%5 SOC value in ECE-15 cycle. (b) ICE and EM power values for 55% SOC. (c) EM speed–torque values for 55% SOC. (d) Specific fuel consumption map for 55% SOC.

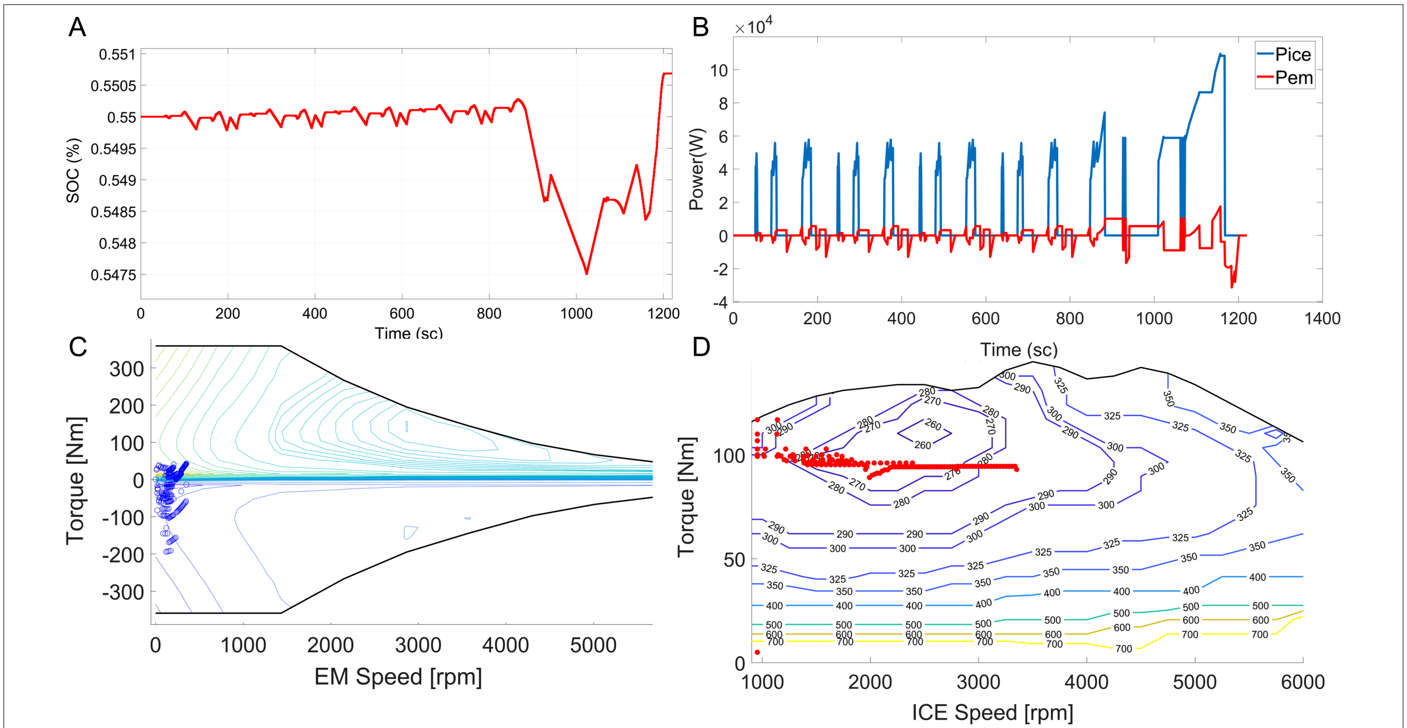

Fig. 9. (a) 55% SOC value in NEDC cycle. (b) ICE and EM power values for 55% SOC. (c) EM speed–torque values for 55% SOC. (d) Specific fuel consumption map for 55% SOC.

In Fig. 8a, the variation of the SOC value over time in the EUDC cycle is expressed. It is seen that the SOC value decreases until the 200th second and then increases. The decrease in SOC indicates that the speed value is low and the EM is used. The power values of EM and ICE are given in Fig. 8b. In this cycle, it has been observed that ICE works more than EM. Also, where ICE power is high, EM produces negative power and works as a generator. When Fig. 8c is examined, it is seen that the EM is operated more as a generator in this cycle by generating torque in the negative region. In Fig. 8d, it is shown that the specific fuel consumption values are clustered at the optimum points.

The results of the rule-based control algorithm are shown in Fig. 9 when the SOC value is 55% in the NEDC cycle. Fig. 9a shows the charging and usage of the battery according to the speed changes in the cycle. Because of the high velocity at the end of the NEDC cycle, EM is used as a generator and charges the battery. Power values of ICE and EM are given in Fig. 9b. The EM is used when the speed is low, and ICE is used at high speeds It is seen in Fig. 9b that the EM produces more negative power due to the critical charge value of the battery being chosen as 55%. This allows the EM to operate as a generator according to the rule-based control method. In addition, the fact that the operating points of the EM are located in the parts containing negative torque points in Fig. 9c shows that it works more as a generator. Fig. 9d shows the amount of fuel that ICE has released into the atmosphere per unit time. Here, it is shown that fuel savings are achieved by operating the ICE at the points with the least fuel consumption.

This article is examined fuel consumption in EUDC, NEDC, and ECE-15 driving cycles, which are recommended rule-based energy algorithms to reduce fuel consumption. Table III shows how much fuel the conventional vehicle and the PHEV with a 65% SOC and 55% SOC value consumes on average at 100 km. It is seen that the rule-based algorithm gives good results in fuel consumption compared to conventional vehicles in Table III. Additionally, according to the research of [17], the fuel consumption is 5.4 L/100 km in the EUDC cycle with a fuzzy algorithm, while fuel efficiency is 3.6 L/100 km with a 65% SOC in the proposed algorithm. Therefore, the rule-based algorithm reduces fuel emissions by operating the ICE at optimum points.

V. CONCLUSION

In this study, a new rule-based and battery-priority fuel consumption control method has been proposed in order to optimally operate the ICE efficiency of the PHEV. The proposed method keeps the SOC value in control and the drive system at the optimum value. For this purpose, eleven different rules have been established for the proposed control method, and their use in NEDC, ECE-15, and EUDC driving cycle conditions has been examined. In this study, two different simulation studies were carried out according to the critical SOC battery. Battery values 55% and 65% close to minimum and maximum values were selected, and it was observed how the fuel consumption of the vehicle changed at different SOC values. The PHEV has a 65% SOC value, fuel efficiency was achieved 35.7% in the NEDC driving cycle, 50.1% in the EUDC cycle, and 52.3% in the ECE-15 cycle. Moreover, the PHEV with a SOC value of 55%, fuel efficiency was achieved 29.3% in the ECE-15 driving cycle, 17.6% in the NEDC driving cycle, and 9.6% in the EUDC cycle. Thanks to the proposed control method, not only were fuel consumption minimized and carbon emissions reduced, but the highest level of driving systems, continuous control of critical battery status, and optimum efficiency of the ICE were also ensured. In future studies, we plan to experimentally test these theoretical results in real time.

Peer-review: Externally peer-reviewed.

Author Contributions: Concept – Y.S.A., N.B.; Design – Y.S.A.; Supervision – N.B., H.T.; Materials – N.B., H.T.; Data Collection and/or Processing – Y.S.A., N.B.; Analysis and/or Interpretation – Y.S.A., N.B.; Literature Review – Y.S.A.; Writing – Y.S.A.; Critical Review – N.B., H.T.

Acknowledgments: This study was supported by TÜBİTAK ARDEB 1003 Engineering Research Group with project number 216M252 and titled "Development of Fuel Efficiency Increasing and Innovative Technologies for Internal Combustion Motor Vehicles." In addition, this study was supported by the Scientific Research Projects Coordination Unit of Istanbul University—Cerrahpaşa with project number 33416 and titled "Development of Innovative Technologies for Hybrid Vehicles."

Declaration of Interests: The authors have no conflict of interest to declare.

Funding: The authors declared that this study has received no financial support.

REFERENCES

1. M. Akil, E. Dokur, and R. Bayindir, "A coordinated EV charging scheduling containing PV system," *Int. J. Smart Grid Clean Energy* vol. 6, no.3, pp.65–71, 2022.
2. E. Dokur, N. Erdogan, and S. Kucuksari, "EV fleet charging load forecasting based on multiple decomposition with CEEMDAN and swarm decomposition," *IEEE Access*, vol. 10, pp. 62330–62340, 2022. [CrossRef]
3. W. Shabbir, and S. A. Evangelou, "Threshold-changing control strategy for series hybrid electric vehicles," *Appl. Energy*, vol. 235, pp. 761–775, 2019. [CrossRef]
4. N. Ding, K. Prasad, and T. T. Lie, "Design of a hybrid energy management system using designed rule-based control strategy and genetic algorithm for the series-parallel plug-in hybrid electric vehicle," *Int. J. Energy Res.*, vol. 45, no. 2, pp. 1627–1644, 2021. [CrossRef]
5. H. Son, and H. Kim, "Development of near optimal rule-based control for plug-in hybrid electric vehicles taking into account drivetrain component losses," *Energies*, vol. 9, no. 6, p. 420, 2016. [CrossRef]
6. Z. Chen, R. Xiong, K. Wang, and B. Jiao, "Optimal energy management strategy of a plug-in hybrid electric vehicle based on a particle swarm optimization algorithm," *Energies*, vol. 8, no. 5, pp. 3661–3678, 2015. [CrossRef]
7. H. Son, H. Kim, S. Hwang, and H. Kim, "Development of an advanced rule-based control strategy for a PHEV using machine learning," *Energies*, vol. 11, no. 1, p. 89, 2018. [CrossRef]
8. X. Li, and S. A. Evangelou, "Torque-leveling threshold-changing rule-based control for parallel hybrid electric vehicles," *IEEE Trans. Veh. Technol.*, vol. 68, no. 7, pp. 6509–6523, 2019. [CrossRef]
9. B. V. Padmarajan, A. McGordon, and P. A. Jennings, "Blended rule-based energy management for PHEV: System structure and strategy," *IEEE Trans. Veh. Technol.*, vol. 65, no. 10, pp. 8757–8762, 2016. [CrossRef]
10. J. Peng, H. Fan, H. He, and D. Pan, "A rule-based energy management strategy for a plug-in hybrid school bus based on a controller area network bus," *Energies*, vol. 8, no. 6, pp. 5122–5142, 2015. [CrossRef]
11. J. Peng, H. He, and R. Xiong, "Rule based energy management strategy for a series-parallel plug-in hybrid electric bus optimized by dynamic programming," *Appl. Energy*, vol. 185, pp. 1633–1643, 2017. [CrossRef]
12. Z. Zhang, T. Zhang, J. Hong, H. Zhang, and J. Yang, "Energy management optimization of master–slave hybrid electric vehicle under rule-based control strategy," *Energy Technol.*, vol. 10, no. 10, p. 2200630, 2022. [CrossRef]
13. H. He, Y. Shou, and H. Wang, "Fuel economy optimization of diesel engine for plug-in hybrid electric vehicle based on equivalent operating points," *Control Eng. Pract.*, vol. 123, 2022. [CrossRef]
14. D. Zhu, E. Pritchard, S. Dadam, V. Kumar, and Y. Xu, "Optimization of rule-based energy management strategies for hybrid vehicles using dynamic programming," *Combust. Engines*, vol. 184, no. 1, pp. 3–10, 2021. [CrossRef]
15. Y. Arıkuşu, M. K. Kazaklı, S. İn, and H. Tiryaki, "Determination of inputs and outputs in hybrid control unit design and designing of fuzzy logic controller," *J Sci Technol*, no. 1, pp. 19–24, 2020. (In Turkish: Hibrit Kontrol Ünitesi Tasarımında Giriş ile Çıkışların Belirlenmesi ve Bulanık Mantık Kontrolörün Oluşturulması, *Bilim, Teknoloji ve Mühendislik Araştırmaları Dergisi*, vol. 1, no. 1, pp. 19–24).
16. K. Ma, Z. Wang, H. Liu, H. Yu, and C. Wei, "Numerical investigation on fuzzy logic control energy management strategy of parallel hybrid electric vehicle," 10th International Conference on Applied Energy, Hong Kong, China, 22–25 August 2018. [CrossRef]
17. F. Sher *et al.*, "Novel strategies to reduce engine emissions and improve energy efficiency in hybrid vehicles", *Cleaner Engineering and Technology*, vol. 2, 2021. [CrossRef]
18. M. Suhail, I. Akhtar, S. Kirmani, and M. Jameel, "Development of progressive fuzzy logic and ANFIS control for energy management of plug-in hybrid electric vehicle,", in *IEEE Access*, vol. 9, pp. 62219–62231, 2021. [CrossRef]
19. C. Saju, P. A. Michael, and T. Jarin, "Modeling and control of a hybrid electric vehicle to optimize system performance for fuel efficiency," *Sustain. Energy Technol. Assess.*, vol. 52, 2022:/[CrossRef]
20. A. Prasanthi, H. Shareef, M. Asna, A. A. Ibrahim, and R. Errouissi, "Optimization of hybrid energy systems and adaptive energy management for hybrid electric vehicles," *Energy Convers. Manag.*, vol. 243, pp. 114357, 2021. [CrossRef]
21. S. Aurelio, *"Trends and Hybridization Factor for Heavy-Duty Working Vehicles, Hybrid Electric Vehicles, Teresa Donateo"*. IntechOpen, 2017. [CrossRef]
22. L. Guzzella, and A. Amstutz, *The QSS Toolbox Manual*. Zürich, Switzerland: institute for dynamic systems and control, department of mechanical and process engineering, 2005.

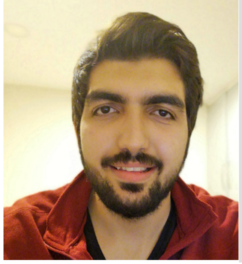

Yılmaz Seryar ARIKUŞU was born in Mersin in 1992. He received his BSc degree in electrical and electronic engineering from Isık University in 2015. He completed his MSc degree in electrical and electronics engineering from Istanbul Bilgi University in 2018. He is currently a research assistant at the Electrical Engineering Department of Manisa Celal Bayar University. He is also PhD candidate in electrical and electronics engineering at Istanbul University—Cerrahpaşa. He is member of IEEE Students. His research interests are automatic control systems, hybrid electric vehicles, artificial intelligence, robust control, control system design, and metaheuristic optimization algorithms.

Nevra BAYHAN was born in Istanbul. She received her BSc degree (Hons) and MSc degree in electrical and electronics engineering from Istanbul University in 1997 and 2001, respectively. She completed her PhD in control and automation engineering at Istanbul Technical University in 2008. She is currently an assistant professor at the Electrical and Electronics Engineering Department of Istanbul University—Cerrahpaşa. From 2017 to 2022, she has worked as the head of Main Scientific Branch Control and Command Systems of Electrical and Electronics Engineering Department, Istanbul University—Cerrahpaşa. Her research interests include automatic control systems, control systems design, artificial intelligence, metaheuristic optimization algorithms, time-delay systems, heat transfer in thermoelectric power generation (TEG) and thermoelectric cooling (TEC) systems, system modeling, fuzzy control, low order controller design, renewable energy systems, robust control, digital control systems, hybrid electric vehicles, and control of systems with parameter uncertainties.

Hasan TİRYAKİ was born in Denizli in 1980. He received his BSc and MSc degrees in electrical and electronics engineering from Kirikkale University in 2002 and 2005, respectively. He received his PhD degree in electrical and electronics engineering from Istanbul University in 2013. From 2016 to 2022, he worked as an assistant professor at Istanbul University—Cerrahpaşa Faculty of Engineering, Department of Electrical and Electronics Engineering. Since 2022, he has been working as an associate professor. In addition, he has worked as the head of Main Scientific Branch Control and Command Systems of Electrical and Electronics Engineering Department, Istanbul University—Cerrahpaşa from 2022. His research interests are electrical cars, control systems, automation, renewable energy, and power generation, transmission, and distribution.